



Showcasing research from Dr Satyasankar Jana's laboratory, Institute of Sustainability for Chemicals, Energy and Environment (ISCE<sup>2</sup>), Agency for Science, Technology and Research (A\*STAR), Singapore.

Polymer material innovations for a green hydrogen economy

This review explores advancements in polymer materials for the green hydrogen economy, covering polymer membranes in hydrogen production, utilization and storage, including solid carriers, applications in hydrogen infrastructure and future research directions.

As featured in:



See Satyasankar Jana, Anbanandam Parthiban *et al.*, *Chem. Commun.*, 2025, **61**, 3233.



Cite this: *Chem. Commun.*, 2025, **61**, 3233

## Polymer material innovations for a green hydrogen economy

Satyasankar Jana, \* Anbanandam Parthiban \* and Wendy Rusli

Polymeric materials are ubiquitous in modern life. Similar to many other technological applications, polymer materials are essential in advancing the green hydrogen economy, offering solutions for hydrogen production, storage, transport, and utilization. In production, polymeric proton exchange membranes in water electrolyzers enable efficient green hydrogen generation using renewable energy. Polymer-based composite tanks provide lightweight, high-strength on-board storage options for vehicles, enhancing safety and reducing costs. Polymeric proton exchange membranes in fuel cells efficiently convert hydrogen into electricity. Polymers also support hydrogen infrastructure with corrosion-resistant, durable pipelines, distribution ports and as hydrogen sensors. Additionally, porous and reversible hydrogenated-to-dehydrogenated forms of polymers show promise for material-based storage systems. This review highlights the role of polymer materials, their current advancements supporting a green hydrogen economy as a solution for a low-carbon future and future research directions.

Received 29th October 2024,  
 Accepted 14th January 2025

DOI: 10.1039/d4cc05750c

[rsc.li/chemcomm](http://rsc.li/chemcomm)

*Institute of Sustainability for Chemicals, Energy and Environment (ISCE<sup>2</sup>), Agency for Science, Technology and Research (A\*STAR), 1 Pesek Road, Singapore 627833, Republic of Singapore. E-mail: [satyasankar\\_jana@isce2.a-star.edu.sg](mailto:satyasankar_jana@isce2.a-star.edu.sg), [a\\_parthiban@isce2.a-star.edu.sg](mailto:a_parthiban@isce2.a-star.edu.sg)*

### 1. Introduction

The urgent need to limit the rise in global temperatures due to fossil fuel-induced global warming has highlighted a few viable alternative energy sources. Among the various non-carbon-based options, hydrogen stands out as a clean, reliable, and potentially sustainable energy vector.<sup>1</sup> It is increasingly seen as



**Satyasankar Jana**

*Dr Satyasankar Jana is a Principal Scientist at the Institute of Sustainability for Chemicals, Energy, and Environment (ISCE<sup>2</sup>), A\*STAR, Singapore. He completed MTech in Materials Science and Engineering at the Indian Institute of Technology (IIT), Kharagpur, India and earned his PhD in Polymer Chemistry from the University of Strathclyde, Glasgow, UK. Later he conducted his post-doctoral research work at the University of Liverpool, UK. Dr Jana's current research focuses on*

*controlled radical polymerization, non-isocyanate polyurethane along with the development of other sustainable and functional polymers. His work extends to anti-fouling, solar-reflective cool, emission-free, autonomous-friendly, and hydrogen embrittlement-resistant coating technologies.*



**Anbanandam Parthiban**

*Dr Anbanandam Parthiban is a Principal Scientist at the Institute of Sustainability for Chemicals, Energy and Environment (ISCE<sup>2</sup>) under the Agency for Science, Technology and Research (A\*STAR), Singapore. After obtaining a PhD in the area of polymer science at the Indian Institute of Technology, Madras, India he worked as a post-doctoral fellow at the Max-Planck Institute for Polymer Research, Mainz in Germany. Later, he joined corporate R&D in India and was involved in*

*the development of lubricants, particularly lubricating greases and additives. Then he joined A\*STAR and has been designing monomers, polymers, polymerization reactions centred around sustainability and resource circularity for various applications.*



## Highlight



Fig. 1 Hydrogen in different colours depending on its source and production processes and contribution of a green hydrogen economy to advance different United Nations' SDGs.

key to fostering sustainable development and achieving zero emissions for both industry and society worldwide. Hydrogen possesses significantly higher gravimetric energy density ( $120\text{--}142\text{ MJ kg}^{-1}$ ) compared to many other common fuels of gasoline ( $44\text{--}46\text{ MJ kg}^{-1}$ ) or natural gas ( $42\text{--}55\text{ MJ kg}^{-1}$ ) and coal ( $10\text{--}25\text{ MJ kg}^{-1}$ ).<sup>2</sup> It is widely anticipated that hydrogen will play a pivotal role in energy storage, heating, and transportation across a broad spectrum of applications, including cars, trucks, trains and airplanes. Beyond these uses, hydrogen can serve as a chemical feedstock, aid in the production of synthetic fuels, and be converted back to electricity *via* fuel cells or combustion at power plants.

The societal-scale integration of hydrogen production, storage, transportation and utilization is referred to as the hydrogen economy. Although hydrogen is one of the most abundant elements in nature, over 96% of current global hydrogen production ( $88\text{ Mt year}^{-1}$ ) is derived from the steam reforming of fossil fuels such as natural gas, oil, and coal, with CO<sub>2</sub> emission as a byproduct.<sup>3</sup> To address this, a greener alternative involves producing “green hydrogen” (Fig. 1) *via* water electrolysis powered by renewable energy sources like solar and wind. In this review, we focus on the hydrogen economy that integrates renewable energy systems, which can be referred to as

the green hydrogen economy.<sup>3,4</sup> The development of a green hydrogen economy is envisioned to significantly contribute to several United Nations Sustainable Development Goals (SDGs), particularly SDG 7 (ensuring access to affordable, reliable, sustainable, and modern energy for all) and SDG 13 (urgent action to combat climate change and its impacts).<sup>5</sup>

Despite the natural abundance of elemental hydrogen, its presence as molecular hydrogen in Earth's atmosphere is nearly non-existent. As a result, hydrogen must be produced through various artificial processes to be used as a fuel. Hydrogen possesses several unique characteristics. As the smallest and lightest diatomic molecule, it has an extremely low boiling point ( $-253\text{ }^{\circ}\text{C}$ ), making the liquefaction and transportation of liquid hydrogen energy-intensive. Additionally, one of the major challenges of using hydrogen as a fuel is its low volumetric energy density. Liquid hydrogen has a volumetric energy density of  $<10\text{ MJ L}^{-1}$ , significantly lower than gasoline, which possesses an energy density of  $32\text{ MJ L}^{-1}$ .<sup>2</sup> The challenge becomes even more pronounced under standard atmospheric conditions (1 bar and  $25\text{ }^{\circ}\text{C}$ ), where hydrogen's volumetric energy density is drastically lower than that of gasoline, diesel, and jet fuel, by factors of approximately 3200, 3700, and 3600, respectively.<sup>2b</sup> This necessitates storing hydrogen gas at extremely high pressures, often exceeding 350 bar, to achieve practical energy densities. Due to these factors, the storage and transportation of hydrogen require highly specialized systems designed to handle its unique physical and chemical properties.

Hydrogen is a highly flammable gas and due to its small molecular size, it is also highly permeable. This makes it more prone to leakage through different materials compared to other fuel gases. Another critical challenge is its reactivity with metal-based infrastructure commonly used for energy transportation. Hydrogen can cause metal degradation through a phenomenon known as hydrogen embrittlement (HE) or hydrogen-induced corrosion, which compromises the structural integrity of materials such as steel and aluminum.<sup>6</sup> This poses significant safety concerns for hydrogen storage and transportation using metal based infrastructure. Moreover, hydrogen has recently been classified as a secondary greenhouse gas.<sup>7</sup> While hydrogen itself does not have a direct global warming effect, it interacts with airborne chemicals in ways that extend the atmospheric lifetime of methane, a potent greenhouse gas, and increase the production of ozone, another greenhouse gas. Recent research estimates the global warming potential (GWP) of hydrogen over a 100-year time horizon to be 11–17, which is quite significant (for comparison, the GWP of CO<sub>2</sub> is 1 and that of methane is 28).<sup>7</sup> Therefore, preventing hydrogen leakage is crucial to mitigating its environmental impact, especially as the world seeks to expand its use. In brief, the vision of a green hydrogen economy faces several materials challenges,<sup>2,4a</sup> requiring significant advancements in science and technology across various stages including production, storage, transportation, infrastructure, and usage before hydrogen can be fully integrated into strategies to achieve net-zero emissions.

Polymeric materials are ubiquitous in modern life, finding applications in everything from personal care, hygiene



Wendy Rusli

sustainable and circular polymers, colloids, particles science, encapsulation and coatings.

Mr Wendy Rusli is a Lead Engineer at the Institute of Sustainability for Chemicals, Energy and Environment (ISCE<sup>2</sup>) under the Agency for Science, Technology and Research (A\*STAR), Singapore. He completed his B. App. Sci. in industrial chemistry and MSc in organic chemistry at the Universiti Sains Malaysia (USM). His research focuses on free radical polymerization, polymerization kinetics and polymer reaction engineering. His current research activities include





## Highlight

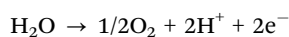
development of PEMWEs in the megawatt (MW) range, from 10 to 35 MW.<sup>9</sup> In PEMWEs, the proton exchange membrane (PEM) acts as a solid polymer electrolyte. The solid polymer electrolyte selectively allows protons to pass through the membrane and at the same time prevents the crossover of gases.

The proton conductivity of widely used commercial Nafion (Fig. 3c) membranes is 0.1 S cm<sup>-1</sup>. Nafion membranes are capable of reaching a maximum current density of 2 A cm<sup>-2</sup> at 1.7–2.05 V.<sup>10</sup> However, fluorine contamination risk is associated with Nafion membranes. In addition, its low glass transition temperature (*T<sub>g</sub>*) of 67 °C causes water loss associated reduction in proton conductivity above 100 °C.<sup>11</sup> A high *T<sub>g</sub>* (127 °C) fluorosulfonic acid membrane commercially known as Aquivion (Fig. 3b) enables it to operate at 120 °C. Physical modification such as biaxial stretching has been employed to reduce the thickness of the Nafion membrane to lower ohmic resistance noticed in thick membranes.<sup>12</sup> Blending of Nafion with inorganic oxides improved characteristics like durability at high temperature, mechanical stability and water retention capability. Inorganic fillers like SiO<sub>2</sub> enabled the operating temperature of Nafion to increase from 80 °C to 120 °C.<sup>13</sup> A 40% reduction in permeability of hydrogen gas was achieved by incorporating impermeable hexagonal boron nitride sheets into Nafion.<sup>14</sup> Interphase separation in Nafion membranes was prevented by blending it with polybenzimidazole (PBI).<sup>15</sup>

Unlike the perfluorosulfonic acid-based PEMs, hydrocarbon-based membranes have some advantages such as high *T<sub>g</sub>*, improved barrier properties against gases and liquids and importantly tailor-made structures to achieve performance requirements. However, the proton conductivity of poly(ether sulfone) based PEM is only 69 mS cm<sup>-1</sup> at 80 °C vs. 100 mS cm<sup>-1</sup> for Nafion based membranes.<sup>16</sup> A higher current density of 3.5 A cm<sup>-2</sup> was reported for sulfonated poly(phenylene sulfone) (sPPS, Fig. 3c) which is higher than the 1.5 A cm<sup>-2</sup> observed for Nafion at 1.8 V. This was because of the reduced gas crossover and lowered high-frequency resistance.<sup>17</sup> However, in the presence of large quantities of water, membrane softening led to degradation of the membrane, affecting its durability. Achieving durability is a challenge in hydrocarbon-based PEMs and because of this reason, perfluorosulfonic acid membranes are preferred.

The reaction that occurs in PEMWEs involves the splitting of water into H<sub>2</sub> and O<sub>2</sub> by an electric current. A reduction occurs at the cathode to produce H<sub>2</sub>, and this process is known as the hydrogen evolution reaction (HER). Likewise, an oxidation occurs at the anode producing O<sub>2</sub> and this process is called the oxygen evolution reaction (OER). The OER, HER and the overall electrolysis reaction that take place on PEMWEs are given below:

Oxygen evolution reaction (OER)



Hydrogen evolution reaction (HER)



Overall reaction



There are many challenges facing PEMWEs. Some of these are listed below: requirement for corrosion resistant materials as stack components that are durable under acidic conditions, sluggish reaction kinetics in acidic environments,<sup>18</sup> ohmic losses during operation,<sup>19</sup> high production cost of H<sub>2</sub>,<sup>20</sup> high cost of installation,<sup>21</sup> and requirement of noble metals as catalysts. The demands of operating conditions can be noticed by the fact that high temperature water electrolyzers are operated above 100 °C and at pressures exceeding 350 bar in completely hydrated conditions. This requires PEMs with high robustness to withstand the harsh operating environment.<sup>22</sup> Because of this issue, PEMWE that is capable of performing for 50 000 hours is yet to be realized.

One of the key advantages of AEMWE is its ability to function with non-noble metal based electrocatalysts. However, unlike PEMWEs, AEMWEs are still at the research and development stage and commercialization is a long way away. This is mainly because of the requirement of long-term durability at 1 A cm<sup>-2</sup> for >3000 h. One major factor affecting the durability of anion exchange membranes is intrinsic in nature. The functionality that is the source of its conductivity in AEM is ammonium hydroxide. Quaternary ammonium compounds are unstable due to their tendency to undergo degradation or elimination by the Hofmann mechanism. Although researchers have developed an impressive range of anion exchange membranes as shown in Section 7 of this article (Fig. 14) these structural modifications primarily address improving the hydrolytic stability of the membranes by avoiding ether linkages (C–O–C) and introducing tertiary carbon atoms in the polymer. However, the fundamental nature of degradation initiated by quaternary ammonium groups is hard to eliminate due to the aforementioned intrinsic character.

In AEMWEs, water is split into H<sub>2</sub> and hydroxide anions. Then the hydroxide anions are oxidized to O<sub>2</sub> after transferring from the cathode to anode by a separator. The reactions that occur at the cathode, anode and the overall reaction are summarized in the following equations:

Reaction occurring at the cathode



Reaction occurring at the anode



Overall reaction



Like PEMWEs, photoelectrochemical (PEC) water splitting is another method of producing hydrogen sustainably from water. The advantage of the PEC process lies in its ability to emit the lowest global warming potential (GWP) per kg of H<sub>2</sub> produced which is 1.0 kg CO<sub>2</sub> per kg of H<sub>2</sub>. In comparison, wind-based PEM water electrolysis has the GWP of 4.0 kg CO<sub>2</sub> per kg of H<sub>2</sub>



and photovoltaic-solar-based PEM water electrolysis has the GWP of 1.5 kg CO<sub>2</sub> per kg of H<sub>2</sub>.<sup>23</sup>

In the PEC process, conducting polymers are used as photo-active electrode materials. Conjugated polymers offer benefits such as easily adjustable energy bands, and broad absorption range combined with tunable molecular structures.<sup>24</sup> Polyaniline,<sup>24</sup> polypyrrole,<sup>25</sup> and poly(3,4-ethylenedioxy thiophene) (PEDOT)<sup>26</sup> are some of the widely studied conducting polymers as photoactive electrodes in PEC devices. Carbon nitrides, covalent triazine frameworks and covalent organic frameworks (COFs) have also been studied as organic polymeric photocatalysts.<sup>27</sup>

Conjugated microporous polymers have been reported to generate hydrogen by water splitting using visible light.<sup>28</sup> Since UV light accounts for only 3% of energy available in the solar spectrum at ground level, photo electrocatalysts that are active under visible light are preferred. A one-dimensional conducting polymer, poly(diphenylbutadiyne), obtained by photopolymerization through a soft templating approach showed high photo electro catalytic activity under visible light without the aid of sacrificial reagents or precious metal cocatalysts.<sup>29</sup> Another "conjugated polymer nanocrystal" based on poly[1,6-di(*N*-carbazolyl)-2,4-hexadiene] (PDCHD) showed high effectiveness under visible light.<sup>30</sup> Conjugated polymeric systems composed of donor and acceptor units are receiving considerable interest in the area of photoelectrocatalysis.<sup>31</sup> Fig. 4 show the chemical structure of various donors that are either fully carbon based or containing heteroatoms like N, O and S. Fig. 5 shows the chemical structure of selected linear polymers that are



Fig. 5 Chemical structure of commonly used polymeric acceptors.

commonly used as acceptors. It may be noted that in PEM devices these donor and acceptor moieties are part of separate polymer films or are constituents of the same polymer chain.

A sacrificial agent free overall water splitting in a PEC process on a large scale is difficult to achieve because of various reasons. First and foremost, the electronic band structure of the conducting polymer should be aligned with the potentials of proton reduction to hydrogen and oxidation of water to oxygen.<sup>32</sup> In addition, the H<sub>2</sub> and O<sub>2</sub> gases produced as a result of water splitting should be sufficiently isolated to prevent its recombination.<sup>33</sup> Apart from these, there are challenges for making the conducting polymers in large scale cost effectively. Inherent defects and durability of these polymers are some of the other issues.<sup>31</sup>

In summary, enhancing energy conversion efficiency, ensuring long-term stability along with achieving economic viability are the three critical challenges that need to be addressed to practically implement PEC systems.<sup>34</sup>

### 3. Porous polymers for materials-based hydrogen storage

Polymers tend to form pores of different nature due to the way the polymer chains arrange and pack in bulk. By introducing features like backbone rigidity, distortion in the polymer backbone, pendant functional groups, *etc.*<sup>35</sup> it is possible to tune the nature of the abovementioned pores. A ladder type polymer that formed micropores intrinsically and hence was called polymer of intrinsic microporosity (PIM) was introduced in 2004.<sup>36</sup> The chemical structure of this PIM-1 is shown in Fig. 6.

This polymer was originally studied for gas separation properties. Subsequently, this polymer was explored for its suitability to store hydrogen gas. PIM-1 absorbed 1.45 wt% of hydrogen at 10 bar of hydrogen pressure at 77 K. The hydrogen uptake properties of PIM-1 were sensitive to high temperature treatment.<sup>37</sup> PIM-1 was also subjected to low temperature treatment to check its ability to withstand elastic deformations that could occur within the high pressure hydrogen storage tanks.<sup>38</sup> In a long term stability study conducted over 400 days,



Fig. 4 Chemical structure of commonly used polymers as (a) fully carbon-based donors, (b) nitrogen containing donors, (c) oxygen containing donors, (d) sulphur containing donors and (e) mixed atom containing donors.





Fig. 6 (a) Porous polymers for hydrogen storage and (b) chemical structure of different polymers of intrinsic microporosity (PIM).

the mechanical properties of PIM-1 remained intact. However, in a statistically significant sample set a decrease in hydrogen storage capacity was noticed.<sup>39</sup> Marginally higher hydrogen storage capacity was reported for PIM-1 modified to MePIM (Fig. 6).<sup>40</sup>

The advances in materials synthesis and in particular organic synthesis have enabled the design, synthesis and evaluation of a diverse variety of soluble and insoluble porous materials for hydrogen storage applications. In this regard, a deeper look into some fundamental issues is necessary to evaluate the suitability of porous polymers for hydrogen storage applications. Many of the developments revolved around enhancing the surface area with tailor made porosity characteristics. However, significant improvements in the surface of materials to enhance attractive forces are required to achieve hydrogen absorption that is relevant for practical use.<sup>41</sup> The hydrogen storage capacity of many of the porous polymers is studied typically at 77 K at less than 5 MPa of hydrogen pressure. However, for automotive applications, the storage capacity should be studied at 298 K under a hydrogen pressure of 50 MPa.<sup>41</sup> In general, for microporous materials, the total volumetric storage gain over compressed hydrogen gas was low. Hence, there is a noticeable change of direction in this field. This is evident from two recent trends. One involves the preparation of composites between PIM and other porous materials like COF and metal organic frameworks (MOF). This approach has the added benefit of enhancing the processability of COFs and MOFs. The other involves an additive approach where organometallic compounds are combined with COFs to enhance hydrogen uptake. In this regard, PIM-1 was blended with PAF-1 (Fig. 6). It should be noted that these blends impact the processability and film properties of PIM-1.<sup>42</sup> PIM-1 was also end-capped with a MOF, MIL-101(Cr), as shown in Fig. 6.<sup>43</sup> In the additive approach, a sequential preparation method in which Pt nanoparticles were



Fig. 7 Chemical structure of MeLi@N-CMP.

prepared first followed by the *in situ* formation of microporous organic polymers was employed to improve the hydrogen uptake of microporous organic polymers.<sup>44</sup>

Lithium doping was used to enhance the hydrogen storage capacity of conjugated microporous polymer (CMP) (Fig. 6) through cation- $\pi$  interaction.<sup>45</sup> In another instance, methyl lithium was used as a dopant in the naphthyl unit containing conjugated microporous polymer to prepare MeLi@N-CMP (Fig. 7).<sup>46</sup> MeLi@N-CMP showed 150% increase in hydrogen uptake over the undoped N-CMP at 77 K and 80 bar and 100% increase over undoped N-CMP at 273 K and 80 bar.

Processing into films and other forms is a major advantage of polymers as is reflected in the studies involving PIM-1. As mentioned before, currently, processing of COFs and MOFs into desired forms is challenging. The approach that involves blending of COFs and MOFs with PIM-1 to improve the processability has severe limitations. Therefore, three-dimensional (3D) printing was attempted to improve the processability of MOFs.<sup>47</sup> In this development, a composite was formed by mixing acrylonitrile butadiene styrene (ABS) copolymer with zinc terephthalate (Zn-TPA) known as MOF-5. 3D printing of composites with concentrations of MOF-5 of 10% or below could be 3D printed. The blending process caused some degradation of MOF-5 and it partially retained the ability to uptake hydrogen.

## 4. Polymeric hydrogen carrier (PHC)

Before diving into PHCs, it is prerequisite to briefly discuss liquid organic hydrogen carriers (LOHCs), as they are highly relevant and currently garner significant interest in the field. LOHCs are organic liquids that can store and release hydrogen through reversible hydrogenation-dehydrogenation reactions.<sup>48</sup> The role of LOHCs in hydrogen transportation, along with examples of common LOHCs, are illustrated in Fig. 8. In such systems, the liquid unsaturated LOHC is heated to a specific temperature in the presence of hydrogen and a catalyst, leading to the formation of a hydrogen-rich hydride/saturated LOHC through an exothermic reaction. Conversely, when the saturated LOHCs are heated to a specific temperature in the presence of





Fig. 8 (a) Role of LOHCs on hydrogen transportation and (b) example of a few common LOHCs in their hydrogenated and dehydrogenated forms.

appropriate catalyst, they release hydrogen gas and form hydrogen-lean, unsaturated LOHCs *via* an endothermic process. LOHC technology holds great promise due to its ability to store large quantities of hydrogen, its compatibility with existing infrastructure, and the absence of hydrogen loss during long-term storage or overseas transportation. For effective use, LOHCs should meet specific criteria, including non-toxicity, low cost, low melting point (< 30 °C), high boiling point (> 300 °C), low dynamic viscosity, high hydrogen storage capacity (> 6 wt%), mild dehydrogenation temperature, and high thermal stability for an extended lifespan.<sup>48</sup> Fig. 8b highlights some widely used LOHCs, along with their dehydrogenated and hydrogenated forms, such as toluene-methylcyclohexane, naphthalene-decalin, dibenzyltoluene-perhydro-dibenzyltoluene, and *N*-ethylcarbazole-dodecahydro-*N*-ethylcarbazole, as well as their hydrogen storage capacities.

In very recent years, polymers with functional groups similar to those in LOHCs, capable of existing in both hydrogenated and dehydrogenated forms, have been investigated as PHCs. The primary advantages of PHCs include their low toxicity, negligible vapor pressure even at high temperatures due to their polymeric nature, reduced contamination of released hydrogen during the dehydrogenation process, high thermal stability, moldability, and ease of handling.

The concept of hydrogenated–dehydrogenated polymer systems, although not initially intended for hydrogen storage, was first explored nearly a century ago by Staudinger *et al.*<sup>49</sup> They hydrogenated polystyrene solution at 200 °C using a nickel catalyst, resulting in poly(cyclohexyl ethylene). The researchers measured the relative viscosities of the polymer solutions before and after hydrogenation, concluding that the unchanged viscosities were due to the covalent bonding in the polymeric structure of polystyrene, rather than secondary binding forces.

This experiment provided critical evidence supporting the covalent nature of polystyrene's repeat units. Kato *et al.* recently revisited the chemistry and successfully produced fully hydrogenated poly(cyclohexyl ethylene) by reacting polystyrene with 10 MPa of hydrogen pressure at 200 °C in the presence of a palladium catalyst.<sup>49c</sup> They also demonstrated that hydrogen could be quantitatively released from hydrogenated polystyrene (poly(cyclohexyl ethylene)) when heated with a platinum catalyst, confirming that polystyrene could function as a PHC.

In 2016, Nishide's group from Waseda University in Japan reported a novel reversible hydrogen capture-release system using a ketone (fluorenone)–alcohol (fluorenol) polymer under milder conditions.<sup>50</sup> They synthesized crosslinked hydrophilic fluorenone/fluorenol polymer networks *via* a cross-linking quaternization reaction involving a bifunctional fluorenone or fluorenol amine derivative (2,7-bis[2-(diethylamino)ethoxy]-9-fluorenone or -fluorenol) and a trifunctional cross-linker (1,3,5-tris(bromomethyl)benzene) at 90 °C (Fig. 9a). Fluorenone, an aromatic ketone, can be electrolytically reduced to fluorenol. After reducing the fluorenone polymer to produce the fluorenol polymer, they studied hydrogen evolution by heating the fluorenol polymer at 80 °C with an iridium catalyst. Remarkably, the rate of hydrogen evolution from the fluorenol polymer was 30 times higher than that of monomeric fluorenol. The hydrogenation–dehydrogenation performance of the fluorenone–fluorenol polymer system remained consistent after 50 cycles. Although the theoretical hydrogen storage capacity (HSC) of the fluorenol polymer is only 0.29 wt%, this research opened new avenues for hydrogen storage beyond traditional small molecule ketone–alcohol systems, which cannot be used as LOHCs due to their volatility. Later, the same group reported a more straightforward synthesis of the fluorenol polymer *via* the polymerization of vinyl fluorenol.<sup>51</sup>

In 2020, Oyaizu's group advanced the fluorenone–fluorenol polymer system by enabling hydrogenation under milder conditions (Fig. 9b).<sup>52</sup> Unlike the earlier electrochemical



Fig. 9 (a) Synthesis of fluorenone polymer, (b) dehydrogenated and hydrogenated forms of fluorenone (orange)–fluorenol (white) polymer sheets, (c) hydrogenation kinetics of fluorenone polymer at 25 °C and 1 atm of hydrogen gas and (d) dehydrogenation kinetics of fluorenol polymer at 95 °C (inset gas chromatography plot of the hydrogen peak).<sup>52</sup> Copyright Wiley 2020.



## Highlight

hydrogenation method reported by Nishide's group,<sup>50</sup> this new approach utilized molecular hydrogen in the presence of an iridium catalyst at ambient conditions.<sup>52</sup> The researchers achieved quantitative conversion for both hydrogenation and dehydrogenation processes (Fig. 9c and d), with gas chromatography confirming the evolution of one equivalent of hydrogen per fluorenone unit. This corresponds to a hydrogen storage capacity of 0.28 wt%, as estimated from the polymer's repeating unit.

As shown in Fig. 8, naphthalene is a well-studied LOHC with high hydrogen storage capacity. However, no studies have been reported on naphthalene-containing polymers for hydrogen storage. Nevertheless, drawing inspiration from the fluorenone-fluorenone system, Nishide and Oyaizu's group explored a quinaldine (QD) polymer as a PHC (Fig. 10).<sup>53</sup> QDs, which are nitrogen-containing heterocycles similar in structure to naphthalene, are commonly found in natural products. QD and its derivatives have been investigated as hydrogen storage materials, with QD capable of storing two hydrogen molecules by forming chemical bonds, resulting in 1,2,3,4-tetrahydroquinaldine (HQD).<sup>54</sup> The N-H bond and adjacent C-H bonds in QD are weaker than the C-H bonds found in carbocycles like naphthalene. Consequently, the HQD ring thermodynamically favours hydrogen release under relatively mild conditions, reverting to QD. In their study, Nishide and Oyaizu's group synthesized QD polymers by reacting amino-QD or amino-HQD with poly(acrylic acid) in a 1:1 molar feed ratio using 4-(4,6-dimethoxy-1,3,5-triazin-2-yl)-4-methylmorpholinium chloride as a condensation

reagent (Fig. 10a).<sup>53</sup> The degrees of substitution for the QD and HQD units in the resulting polymers were 0.51 and 0.53, respectively. Both copolymers were insoluble in water but exhibited hydrophilic properties, absorbing up to 25–35 wt% of water to form gels. The QD-substituted copolymer was electrochemically hydrogenated up to 75%, and it achieved over 90% dehydrogenation when heated to 80 °C in the presence of an iridium catalyst.

The research team further advanced the PHC system by significantly improving the dehydrogenation rate constants of polymers containing other nitrogen heterocyclic compounds. This enhancement was achieved by increasing the number of nitrogen atoms within the aromatic ring and by substituting methyl and phenyl groups on the ring structure. These modifications were successfully applied to poly(vinyl quinoxaline),<sup>55</sup> poly(vinyl dimethylquinoxaline),<sup>55</sup> and poly(vinyl diphenylquinoxaline),<sup>56</sup> as illustrated in Fig. 10.

In recent studies, polymers containing ketone and butanediol groups have been explored for their hydrogenation–dehydrogenation properties, aimed at their application as PHCs.<sup>57</sup> The structures of these polymers are shown in Fig. 11. These PHCs are notable for their simplicity in structure and ease of synthesis. However, the gravimetric hydrogen storage capacity of these polymers remains well below the threshold set by the U.S. Department of Energy. Despite these limitations, the potential of PHCs continues to be an area of active research. The reversible hydrogenation–dehydrogenation of redox-active bistable organic polymers has been recently reviewed by



Fig. 10 (a) Quinaldine copolymer, (b) homopolymers from quinoxaline derivatives and fluorenone used for hydrogenation–dehydrogenation studies and (c) the usual synthesis protocol of monomer and polymer synthesis of quinoxaline and fluorenone.





Fig. 11 Polymer with ketone or hydroxy groups as PHCs.

Oyaizu,<sup>58</sup> Nishide,<sup>59</sup> and Sharifian,<sup>60</sup> which may help to advance this technology.

In general, although PHCs have lower hydrogen storage capacities compared to their low molecular weight counterparts and other LOHCs, their mild dehydrogenation conditions, high dehydrogenation efficiency, and additional benefits being polymers make them highly promising. Polymers such as QD copolymers,<sup>54</sup> poly(vinyl quinoxaline),<sup>55</sup> and polyalanine-acetone systems<sup>57b</sup> are particularly noteworthy for the consideration towards future applications. Developing scalable new polymers that enhance hydrogen storage capacity while retaining these advantages will be a key focus of future research in this field.

## 5. Polymer–metal/metal hydride composite for hydrogen storage applications

Hydride-forming metals such as magnesium (Mg), lithium (Li), sodium (Na), aluminum (Al), nickel (Ni), palladium (Pd), boron (B), and titanium (Ti), along with their alloys and hydrides, exhibit significant potential for hydrogen storage due to their high gravimetric and volumetric hydrogen storage densities, which often surpass those of compressed or liquefied hydrogen gas.<sup>61</sup> However, their application is limited by slow hydrogen regeneration kinetics, prolonged charging and discharging times, and poor stability, particularly with respect to oxygen and moisture tolerance. Recent comprehensive reviews have detailed the hydrogen absorption–desorption processes of these alloys and hydrides.<sup>61a,62</sup>

A promising strategy that has gained considerable attention over the past decade involves the micronization and nanostructuring of these metals and metal hydrides in the presence of polymers (Fig. 12). Polymers offer several key benefits in this context, including (a) reducing the agglomeration of nano- and microparticles, (b) enhancing oxygen and moisture resistance, particularly for highly surface-active nanoparticles, (c) providing dimensional stability by accommodating the volumetric expansion of metal hydrides during hydrogen sorption and desorption, and (d) improving system processability, enabling the production of composites in various geometries such as powders, membranes, and plates.<sup>61a,63</sup> The polymers suitable for these applications must possess high selectivity for hydrogen permeation relative to oxygen, moisture, and other gases,

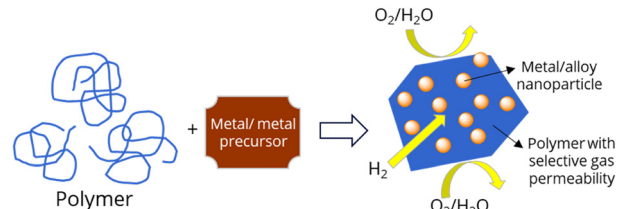


Fig. 12 Schematic representation of polymer-stabilized metal nanoparticle composites as hydrogen storage materials and the enhancement in hydrogen absorption properties of that composite.

as well as exhibit good thermal conductivity, low crystallinity, high thermal stability particularly up to hydrogen desorption temperatures of metal/alloys, sufficient elasticity to accommodate the expansion and contraction of metal particles during hydride formation and decomposition, and preferably elevated glass transition temperature ( $T_g$ ) and crystalline melting points ( $T_m$ ).<sup>61a</sup>

Among the polymers studied, poly(methyl methacrylate) (PMMA) and low- and high-density polyethylene (LDPE and HDPE) have been extensively researched as polymer composites with hydride-forming metals for hydrogen storage. For example, the Urban group reported the development of oxygen- and moisture-resistant PMMA-stabilized Mg nanocrystals of 5 nm, which exhibited a significant improvement in hydrogen uptake (up to 6 wt%) compared to 44  $\mu\text{m}$  Mg particles, which showed no uptake.<sup>64</sup> Other polymers explored in this context include polymethylpentene (TPX), polydimethylsiloxane (PDMS), polystyrene (PS), poly(acrylonitrile–butadiene–styrene) (ABS), polyvinylidene fluoride (PVDF), polylactic acid (PLA), polyethylenimine (PEI), and polyaniline (PANI).<sup>63</sup>

Kubo *et al.* from Japan Steel Works Ltd developed a Ni–Mn–Co alloy polymer composite powder for use in large hydrogen storage tanks, utilizing two commercial silicone resins, ELASTOSIL<sup>®</sup> M4648 and SilGel<sup>®</sup> 612 from Wacker.<sup>65</sup> While the pressure–composition–temperature (PCT) isotherms of both the raw alloy and the polymer composites were found to be similar, the hydrogen reaction rate was slightly slower in the composite, likely due to differing surface characteristics. Although polymer–metal/metal hydride nanocomposites show promise in enhancing air resistance, a strong polymer–metal interaction can negatively affect the hydrogen absorption properties of certain alloys, as the impact of a particular polymer is not universally beneficial across all alloy types.<sup>63</sup>

Several fabrication methods have been explored to produce polymer–metal/metal hydride composites, including solution casting, ball milling, solid-state compacting, cold rolling, hot pressing, and extrusion.<sup>61a</sup> These polymer–metal composites can significantly enhance system performance in hydrogen storage applications. This improvement is attributed to the nanoconfinement effect of the metal nanoparticles and the increased air stability of metal nanoparticles, which are otherwise reactive to oxygen and other gases. To date, most polymers investigated in this context are commercially available materials. However, there is significant potential for developing novel polymer structures with different functionality and architecture



## Highlight

with properties specifically tailored for these specialized applications.

## 6. Polymer materials for hydrogen infrastructure, storage and distribution

This section will highlight the polymer materials used for physical storage of hydrogen, hydrogen infrastructure and distribution.

Hydrogen is the most abundant element in nature, and molecular hydrogen ( $H_2$ ) can be produced from various sources, including water, waste, and fossil feedstocks. However, significant challenges remain in using hydrogen as a future energy carrier for transport vehicles. One major limitation is its low volumetric energy density. At standard conditions (1 bar and 20 °C), the volumetric energy density of hydrogen is  $0.01 \text{ MJ L}^{-1}$ , which is significantly lower than that of gasoline ( $34 \text{ MJ L}^{-1}$ ), diesel ( $38 \text{ MJ L}^{-1}$ ), and jet fuel ( $34.7 \text{ MJ L}^{-1}$ ).<sup>66</sup> To store an equivalent amount of energy, hydrogen requires multiple times the volume (and thus a much larger storage tank) compared to petroleum-based fuels.

Several approaches have been adopted<sup>67</sup> to address this issue using (i) liquefied hydrogen (at  $-253 \text{ °C}$  to  $-259 \text{ °C}$ ); (ii) cryo-compressed hydrogen (at temperatures between  $-233 \text{ °C}$  and  $-193 \text{ °C}$  and pressures around 350 bar) and (iii) as highly compressed gas (at pressures of 700–800 bar at room temperature). Liquefied hydrogen has a volumetric energy density of  $8.5 \text{ MJ L}^{-1}$ . However, its extremely low boiling point ( $-253 \text{ °C}$ ) makes both liquefaction and cryo-compression energy-intensive processes. As a result, high-pressure compressed hydrogen, despite its lower volumetric energy density compared to liquid fuels like gasoline, is generally considered the most practical method for transportation and onboard vehicle storage. For example, at a pressure of 700 bar and 20 °C, gaseous hydrogen has a volumetric energy density of  $5.3 \text{ MJ L}^{-1}$ , while at 350 bar and 20 °C, it is approximately  $2.7 \text{ MJ L}^{-1}$ . The increased pressure allows significantly more gaseous hydrogen to be stored within the same space. However, storing hydrogen at 350 bar instead of 700 bar requires a storage tanker with double the volume to hold the same amount of hydrogen, resulting in a greater overall weight of storage tank. The pressure of 350 bar is used in the tanks of hydrogen trucks or bigger size vehicles, for example, the ones from Hyzon.<sup>66</sup> A loaded 55-ton Hyzon truck needs about 50–70 kg of hydrogen to travel 500 to 600 km. Whereas a smaller sized vehicle like a Hyundai NEXO utilizes 700 bar to store 5 kg of hydrogen in a 125 L tank, which enables it to travel approximately 600 km.<sup>66</sup>

Traditional gas storage tanks (Types I and II, Fig. 13), made of metals and alloys, are unsuitable for high-pressure hydrogen storage for three primary reasons as (i) these metal cylinders cannot withstand the high pressures required for hydrogen storage, especially above 300 bar, (ii) lower gravimetric energy density of the full system when thick wall metal cylinders are used and (iii) metals are susceptible to HE,<sup>66,68</sup> a phenomenon where hydrogen gas is absorbed, diffused, and reacts with the metal. This reaction



Fig. 13 (a) General structure of a vehicle on-board high-pressure hydrogen storage tank (copyright ACS 2023),<sup>69</sup> and (b) different types of hydrogen storage tanks. Liner plastics: HDPE, PP and polyamides/nylons. Composites: glass/carbon fibre composites with epoxy, polyesters, phenolics, polyamides and polyphenylene sulphide.

makes the metal more brittle, reducing its toughness and causing it to crack easily, which increases the risk of hydrogen leakage – a serious safety concern given hydrogen's highly flammable nature and its role as a secondary greenhouse gas.<sup>7</sup>

To address these issues, advanced gas cylinders (e.g., Type III–V in Fig. 13) are used for on-board hydrogen storage in vehicles. These cylinders are typically constructed from carbon or glass fibre-reinforced epoxy composites, making them significantly lighter than thick-walled metal cylinders and more resistant to HE, especially in Type IV and Type V cylinders. The use of fiber-reinforced polymer composites also offers greater design flexibility in storage systems.

Research conducted by Sandia National Laboratories has demonstrated that polymers are not susceptible to HE, unlike metals.<sup>70</sup> This has spurred car manufacturers like Toyota, Honda, Hyundai, and Panasonic to develop innovative on-board storage technologies.<sup>4a</sup> However, it is important to note that while corrosion-resistant metal cylinders and tanks, though expensive, are still in use for on-site hydrogen storage where weight is not a critical factor. Polymers and polymer composites are generally too brittle for storing liquefied hydrogen.

Fiber-reinforced polymer composites offer an exceptionally high strength-to-weight ratio and enhanced thermal and mechanical properties, making them valuable in various industries, including aerospace, marine, automotive, and renewable energy sectors such as wind turbine blades. Commonly used polymer resins for these composites include epoxy, polyester, phenolics, and vinyl esters.<sup>71</sup>



Current research on composite tanks for hydrogen storage focuses on several key areas including (i) development of high-performance composites where researchers are working on creating ultra-strong composites using advanced reinforcing materials like carbon fiber, carbon nanotubes, and graphene,<sup>72</sup> (ii) structural design and characterization where efforts are being made to optimize the structural design and conduct thorough characterization and failure analysis of composite tanks,<sup>73</sup> (iii) application of machine learning (ML) and artificial intelligence (AI) which are being increasingly applied to the design and development of composite tanks, enabling more efficient and effective solutions,<sup>71,74</sup> and (iv) innovation in thermoplastic composites where there is a push to develop new thermoplastic composites that achieve high strength and minimal permeability, particularly for Type V tanks, which do not use polymer liners.<sup>75</sup> This research also aims to improve the recyclability of these materials at the end of their lifecycle.

Polymers and polymer composites play a crucial role in various hydrogen-related applications beyond storage tanks.<sup>75</sup> In the area of hydrogen distribution and delivery, polymers are used in pipelines, piping, and tubing systems that transport hydrogen. Compared to on-board storage tanks, pipelines and tubing systems operate at lower hydrogen pressures (typically less than 100 bar). While current hydrogen pipelines in the United States and Western Europe are primarily made of steel, there is growing interest in using fibre-reinforced polymers and other plastics such as HDPE, polypropylene (PP), and nylons (polyamides) for these purposes. These materials offer advantages in terms of flexibility, corrosion resistance, and ease of installation. Polymers are also extensively used in the manufacturing of valves, pistons, seals, O-rings, and gaskets, which are critical components in hydrogen fuelling stations and vehicle fuelling systems.<sup>75b</sup> The polymers used in these applications include: nitrile rubber (NBR), known for its excellent resistance to oils and fuels, silicone and fluorosilicone rubbers which offer high-temperature stability and flexibility, neoprene which is valued for its good chemical stability and flexibility, ethylene-propylene copolymer (EPDM), widely used for its weather, heat, and ozone resistance, polytetrafluoroethylene (PTFE) recognized for its non-reactive properties and ability to withstand extreme temperatures and polyether ether ether ketone (PEEK) – a high-performance polymer known for its exceptional mechanical and chemical resistance, often used in demanding applications. All these materials are essential for ensuring the safe and efficient distribution and delivery of hydrogen in various systems, contributing to the growing hydrogen economy.

As discussed earlier, polymers and polymer composites offer several advantages over metals, including a superior strength-to-weight ratio, enhanced design flexibility, and significant resistance to HE, owing to their inactivity with hydrogen. However, they also come with certain limitations, one of the most notable being their higher permeability to gases compared to ceramics and some metal alloys.<sup>6</sup>

Gas permeation through polymers can be described as a sequence of three consecutive processes: (i) dissolution/

absorption of gas onto the material's surface, (ii) diffusion of gas molecules through the bulk of the material and finally, (iii) the desorption of gas molecules from the opposite surface of the material. These processes are characterized by three key physical properties: Solubility ( $S$ ) measured in  $\text{mol m}^{-3} \text{ Pa}$ , indicates how much gas can dissolve in the polymer. Diffusivity ( $D$ ) measured in  $\text{m}^2 \text{ s}^{-1}$ , describes how quickly the gas molecules move through the polymer, and permeability ( $P$ ) which is measured in  $\text{mol. m (m}^{-2} \text{ s}^{-1} \text{ Pa}^{-1})$ . Permeability is a function of both solubility and diffusivity, indicating the overall ease with which a gas can permeate through a polymer.

Hydrogen permeability is a critical area of research, especially given the need for high-pressure storage of gaseous hydrogen at and above 350 bar. The permeability of hydrogen, the smallest non-polar molecule, in polymers depends on several factors, including the chemical structure of the polymer, glass transition temperature ( $T_g$ ), crystallinity, temperature of evaluation, crosslink density, degree of polymerization *etc.*<sup>69,76</sup> Polymers or copolymers with more polar groups and a compact structure (lower free volume) like poly vinylidene fluoride (PVDF), polyester, polyamide (PA), and ethylene vinyl alcohol (EVOH) have been reported to have reduced hydrogen permeability.<sup>77</sup> For instance, poly(vinyl alcohol) (PVA), which is rich in hydroxyl groups, demonstrates good hydrogen resistance due to its compact structure, created by strong hydrogen bonds between molecular chains. However, under high humidity, these polar polymers can expand, leading to increased hydrogen permeability.<sup>77a,c</sup>

Studies have shown that amorphous polymers generally exhibit higher hydrogen permeability than crystalline or semi-crystalline polymers. Among various types of polyethylene, HDPE has the lowest hydrogen permeability due to its higher degree of crystallinity, making it an ideal material for storage tank liners, pipelines, and related components. The crystalline regions in semi-crystalline polymers enhance hydrogen barrier properties by increasing the tortuosity of the diffusion path (Fig. 14a). A recent study by Kanetsugi *et al.* highlighted the hydrogen permeability resistance of common polymers used in hydrogen infrastructure, ranking them as follows: PA6 > PA11 > PA12 > HDPE > LDPE > EPDM.<sup>78</sup>

The higher solubility and absorption of nonpolar hydrogen in polymers, particularly in elastomers used for O-rings, seals, and gaskets, can lead to a significant issue known as rapid gas decompression (RGD).<sup>75b,76</sup> RGD occurs when dissolved gas within a material expands rapidly after a sudden release from high pressure. This phenomenon can cause various forms of damage, including cavitation, blistering, cracking, delamination, and rupture. Therefore, it is crucial to evaluate these polymer materials under the necessary conditions before their actual application to ensure they can withstand RGD.

Another effective approach to reduce hydrogen permeability in polymers and polymer composites is to increase tortuosity by incorporating fillers (Fig. 14b). Traditional fillers, such as clay<sup>77a</sup> and glass fibre (used with epoxy),<sup>79</sup> have been widely employed, but current research is focusing on advanced 2D materials. These include graphene<sup>80</sup> (used with PP, epoxy, and



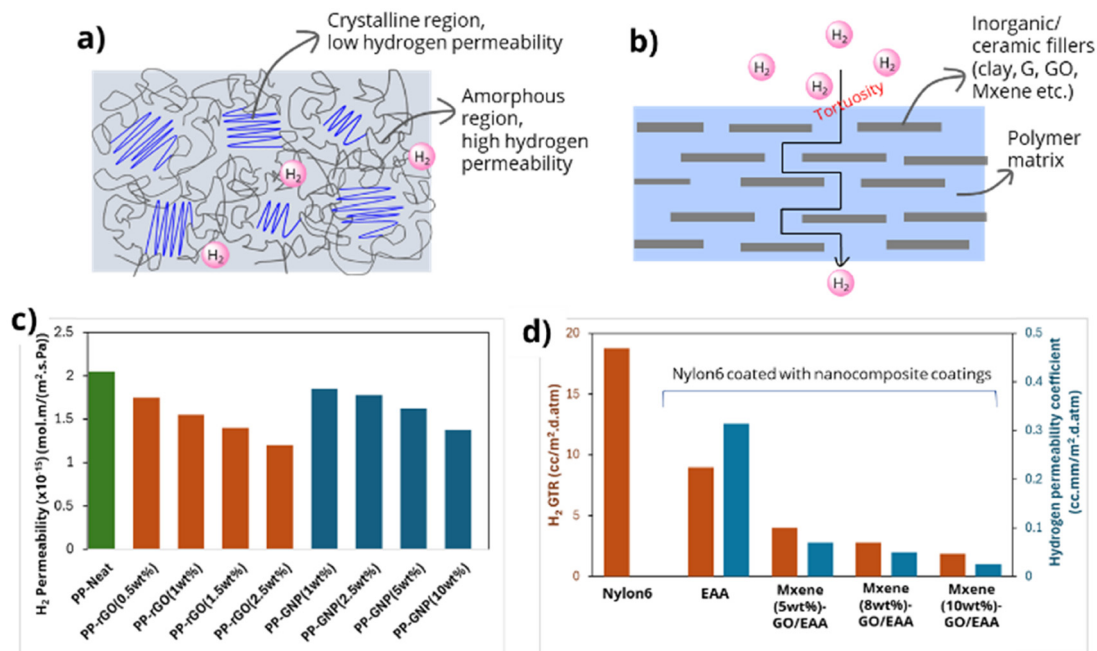


Fig. 14 Hydrogen permeability of (a) a semi-crystalline polymer and (b) a polymer nanocomposite by improving tortuosity. Hydrogen permeability results of (c) PP nanocomposite with rGO and GNP,<sup>80a</sup> and (d) nanocomposite of EAA with GO and MXene.<sup>82</sup>

thermoplastic polyurethane (TPU)), graphene oxide<sup>81</sup> (applied in combinations with polyetherimide (PEI), poly(methacrylic acid), maleic anhydride-grafted PP, and ethylene-vinyl alcohol (EVOH)), and MXene<sup>82</sup> (incorporated with poly(ethylene-co-acrylic acid) (EAA)). Recent studies have shown significant improvements in hydrogen barrier properties using these advanced fillers. For example, the Kinloch group reported a 40% and 30% reduction in hydrogen permeability in PP using reduced graphene oxide (rGO) and graphene nanoplatelets (GNP), respectively (Fig. 14c).<sup>80a</sup> Additionally, Lee's group demonstrated a substantial decrease in hydrogen permeability in a MXene-GO-EAA polymer nanocomposite (Fig. 14d).<sup>82</sup>

Future advancements in polymers and polymer composites for hydrogen-related applications, particularly improving durability in high-pressure environments with minimal hydrogen permeability, will be pivotal for a successful transition from an oil-based economy to a safe and reliable hydrogen-based economy.

## 7. Polymer for hydrogen utilization (membrane in fuel cells)

Fuel cells are some of the most promising devices for clean energy across a variety of applications such as portable devices, residential and transportation. Among different fuel cells, proton exchange membrane fuel cells (PEMFC, Fig. 15a) are an important class due to their versatility, particularly their lower operating temperature and ability to carry high power density. Polymer electrolyte membranes (PEMs) are a vital component of PEMFCs. Fluoropolymers bearing a sulfonic acid group such as Nafion (Fig. 3c) and its modified forms have been widely used in PEMFCs. Some major issues associated with Nafion are

low operating temperature (about 80 °C), the deterioration of mechanical properties with hydration that is essential for conductivity in PEMs, and high methanol crossover. Many alternative polymer systems have been evaluated to replace Nafion. A sulfonated polyphenylene designated as SPP-QP in Fig. 15b has been reported to show superior performance.<sup>83</sup> For example, the maximum operable time for a PEMFC based on SPP-QP was about 10.2 s mg HSP<sup>-1</sup> and the same for Nafion NRE-212 was 3.90 s mg HSP<sup>-1</sup> at a constant current density of



Fig. 15 (a) A proton exchange membrane fuel cell (PEMFC), and (b) chemical structures of some of the sulfonated polymers used as fuel cell membranes.



1 mA cm<sup>-2</sup> and 80 °C. This rechargeable SPP-QP derived PEMFC showed cycleability of at least up to 50 cycles. One major difference and advantage of SPP-QP as compared to other PEMs is its ability to store hydrogen. SPP-QP acts as a hydrogen storable polymer sheet inside the fuel cell thereby avoiding the conventional hydrogen storing media like pressurized hydrogen tank and metal hydrides which are pyrophoric in nature. However, further improvement of SPP-QP is needed in terms of hydrogen storage capacity. SPP-QP, an all polymer rechargeable PEMFC can be considered as next generation PEMFCs. This type of dual functional PEMFC could become attractive if high hydrogen storage capacity and long rechargeability with improved stability of catalyst is achieved.

A push coating method was employed to make mechanically stable membranes from SPP-QP. In this process, SPP-QP was reinforced by a porous polyethylene mechanical support layer.<sup>84</sup> Poly(ether sulfone) bearing a sulfonic acid group has been studied for a long time as a suitable substitute for Nafion membranes for fuel cell applications. The facile preparation and modification of poly(ether sulfone)s have enabled numerous variations in this polymer class. However, cost, ready availability of raw materials and ease of manufacturing polymer and membranes are limiting factors.

A sulfonated polyether sulfone (SPSU) with hydrogen storage capacity of above 500 mA h g<sup>-1</sup> (~1.8 wt% H) of discharge capacity was reported.<sup>85</sup> Cyclic voltammetry studies of the host polymer, SPSU (Fig. 15b) confirmed that ion diffusion occurred within the working electrodes. The charge-discharge efficiency was about 93%, which is comparable with commercial batteries. The starting polymer is commercially available and sulfonation was carried out using chlorosulfonic acid.

The PEMs are subjected to tremendous stress under the operating conditions of PEMFCs. Since these are organic polymers, oxidation stability is vital for the long-term performance of these devices. To enhance hydrolytic stability, it is also useful to avoid C-X linkages in the sulfonated polymer used as PEM. Hence, polyarylene with an all carbon backbone containing densely sulfonated pendant groups (Fig. 15b) was studied.<sup>86</sup> This all-carbon backbone PEM showed high conductivity, excellent dimensional stability and good oxidation stability.

Research efforts are also continuing in the preparation and exploration of composite membranes as PEMs. A nanocomposite membrane was fabricated by incorporating modified (3-aminopropyl)triethoxysilane treated silicon oxide (APTES-SiO<sub>2</sub>) within a poly(vinylidene fluoride) (PVDF) matrix. Sulfonic acid groups were introduced within this nanocomposite membrane by treating it with chlorosulfonic acid.<sup>87</sup> The sulfonated composite membrane showed 50% lower methanol crossover than Nafion. Amphoteric composite membranes made up of sulfonated poly(ether ether ketone) containing imidazole chains with side chain sulfonated poly(ether sulfone) bearing covalently crosslinked perfluoroalkyl chains were studied as PEM.<sup>88</sup> The energy efficiency of this PEM was superior to that of Nafion. It retained 48.6% of charge capacity after 200 charge-discharge cycles at 150 mA cm<sup>-2</sup>.

Anion exchange membranes (AEM) are another type of polymer membranes used in fuel cells. Unlike PEM where

protons *i.e.* H<sup>+</sup> ions are the source of conductivity, hydroxide ions *i.e.* OH<sup>-</sup> are the conducting species in AEMs. In PEM, sulfonic acid provides the protons and in AEMs, the source of hydroxide is ammonium hydroxide. Similar to PEM, AEMs also experience severe oxidative and hydrolytic stress during performance. Therefore, greater attention is directed to design effective durable membranes by using more aromatic groups and linkages free of C-X bonds other than those required for carrying ammonium hydroxide moieties. A comb-shaped poly(terphenyl piperidinium) (PTP) AEM (PTP-OEG 4) that combines crystallinity and local hydrophilic environment of organic cations was studied (Fig. 16a).<sup>89</sup> It showed improved alkaline stability and high current density.

A “windmill” shaped branched poly(aryl piperidine) (TPTP-Pip-OH) (Fig. 16b) bearing terminal hydroxyl groups was prepared and studied.<sup>90</sup> The hydroxyl groups helped to improve the toughness of the membrane enabling the fabrication of self-supported membranes. It exhibited high hydroxide conductivity and retained 87.4% of conductivity for more than 60 days in 2 M NaOH at 80 °C.

A superacid catalyzed polyhydroxyalkylation reaction was used to prepare ether-free fluoropolymer PBPIP-QAPBF (Fig. 16c).<sup>91</sup> This polymer retained 95% of its conductivity after being treated with 2 M NaOH solution at 80 °C for 1080 h.

Poly(aryl-*co*-terphenyl piperidinium)-*x* (PDnTP-*x*) based AEMs (Fig. 16d) with different alkyl spacers (*n* = 0, 1, 2, 6, 10) in the backbone were synthesized and studied.<sup>92</sup> AEMs with long alkyl chains (*n* = 6 or 10) showed improved dimensional stability and low permeability (H<sub>2</sub> permeability 150 mS cm<sup>-1</sup> at 80 °C). The alkaline stability of PDnTP-*x* membranes in 1 M NaOH at 80 °C for 1000 h was excellent. PDnTP-*x* membranes were also stable in Fenton's reagent for 200 h.

Poly(aryl piperidinium) (PAP) anion exchange membranes (AEMs) (Fig. 16e) with a branched structure containing flexible multi-cation crosslinkers have been reported to possess alkaline stability and hydroxide ion conductivity.<sup>93</sup> About 92% of the hydroxide ion conductivity was retained after soaking in 2 M NaOH for 1080 h at 80 °C.

Sulfonic acid and ammonium hydroxide are the source of functionality *i.e.* conductivity in PEM and AEM respectively. In whatever manner the polymer is modified ultimately the loss of function that adversely affects the durability of these devices through the degradation of these functional groups is unavoidable. Therefore, one possibility is replacing the fuel cell stack at fixed, regular intervals to minimize the disruption caused by the inevitable chemical degradation of functionalities and the subsequent loss of performance. Data is key for making such a decision. For this purpose, the durability of a given fuel cell stack needs to be determined under standard conditions. This in turn will provide guidance on the frequency of replacing fuel cell stacks while operating the device.

## 8. Polymer based sensors for detecting hydrogen gas

One major issue with hydrogen is its high flammability. Due to the lower explosion limit of 4% of hydrogen in air, developing





Fig. 16 Chemical structure of (a) PTP-OEG4, (b) TPTP-Pip-OH, (c) ether-free fluoropolymer PBPIP-QAPBF, (d) poly(aryl-co-terphenyl piperidinium) based AEMs PDnTP-x and (e) poly(aryl piperidinium) (PAP) based anion exchange membranes.

sensors to detect hydrogen gas leaks is vital in a green economy comprising of hydrogen-based fuel. Sensors to detect hydrogen have been used commercially for many decades.<sup>94</sup> In general, sensors can be used for detecting hydrogen leaks as well as for quality control purposes such as to check the purity of hydrogen gas. As impurities can poison catalysts used in PEMFCs as well as disrupt membrane function, detecting impurities in H<sub>2</sub> gas is vital for the efficient performance of PEMFCs.

Hydrogen sensors are based on a diverse range of technologies such as acoustic, catalytic, chemiresistive, electrochemical, mechanical, optical, piezoelectric and thermal.<sup>95</sup> In electrochemical hydrogen sensors, polymer electrolytes are used particularly for low temperature operations. In sensors where liquid electrolytes like sulfuric acid are used, it is distributed in polymer membranes such as Teflon. Nafion has also been used to coat reference electrodes used in hydrogen sensors.<sup>96</sup> Solid polymer electrolytes used in sensors are predominantly based on perfluorosulfonic acid membranes. Porous ion exchange polymers,<sup>97</sup> polybenzimidazole (PBI) and sulfonated poly(ether ether ketone) (S-PEEK) (Fig. 17) have also been studied.

Due to its resemblance with PEMFCs, Nafion is preferred as a polymer electrolyte membrane for sensing H<sub>2</sub> gas under conditions relevant for PEMFC operation. A linear sensor response to hydrogen concentration in the range of 200 to 10000 ppm with a sensitivity of 0.0131  $\mu$ A per ppmv H<sub>2</sub> was shown by a sensor based on Pd on carbon fiber that contained 10% loading of Pd.<sup>98</sup> A Nafion-based hydrogen sensor for fuel-cell electric vehicles was fabricated by a conventional hot-pressing method. This sensor responded to H<sub>2</sub> gas in the concentration range of 20–99.99%.<sup>99</sup> A flexible colorimetric hydrogen sensor was fabricated by electrospinning polyacrylonitrile with PdO@ZnO. This was capable of detecting H<sub>2</sub> gas

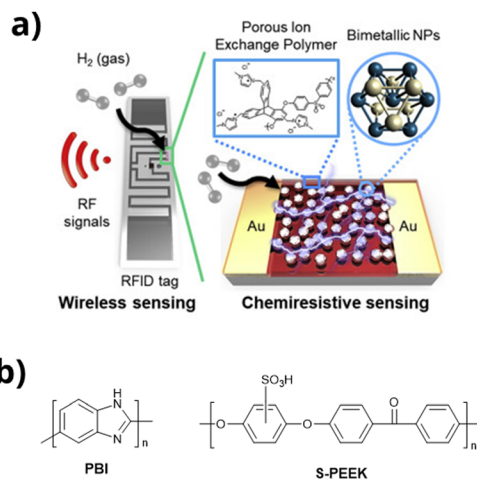


Fig. 17 (a) Polymer-based RFID sensors (Copyright CelPress 2020),<sup>97</sup> and (b) chemical structure of PBI and S-PEEK.

within 2 minutes at 1000 ppm concentration with excellent selectivity.<sup>100</sup> A laminating process was applied to further fabricate into film. Yarn type flexible sensors were obtained by twisting the electrospun fiber followed by coating with polydimethyl siloxane.<sup>101</sup> A hydrogen getter-doped polymer film was studied as an optical H<sub>2</sub> gas sensor.<sup>102</sup> In this a composite film of 1,4-bis(phenylethynyl)benzene with Pd supported on carbon embedded in silicone elastomer was used. Hybrid thin films of vanadium pentoxide (V<sub>2</sub>O<sub>5</sub>) and polypyrrole were fabricated by *in situ* chemical polymerization of the composite V<sub>2</sub>O<sub>5</sub> and pyrrole. The dopant *p*-toluene sulfonic acid helped to improve the sensing performance of the composite film. Minor current changes induced by low hydrogen exposure in 5 to 250 ppm at room temperature were detected in 42 and 37 s respectively by the *p*-toluene sulfonic acid doped vanadium pentoxide–polypyrrole composite film.<sup>103</sup>

In general, some of the requirements of an advanced sensing system are fast, being sensitive and low cost. The explosive nature of hydrogen gas demands a detection technique that is capable of detecting leakages at ppb level in order to prevent major accidents. The sensor should be able to perform under demanding environmental conditions such as varying humidity and temperature along with the interference from other gases. As the usage of hydrogen becomes widespread the sensor technology could further evolve and become well-integrated with modern devices such as smart phones and tablets. Various sensing methods such as those based on colorimetry and other online detecting techniques could combine to make the detection of leakage of hydrogen gas at very low concentrations fast, repeatable and reliable.

## 9. Summary and outlook

This overview highlights the critical roles of polymer materials across various stages of the green hydrogen economy. Polymer electrolyte membranes are pivotal in electrolyzers for hydrogen production and in fuel cells for energy generation. Porous



polymers are promising for physical hydrogen storage, while polymers with reversible hydrogenation properties serve as PHCs. Semi-crystalline polymers and polymer nanocomposites, with low hydrogen permeability, are essential for safe hydrogen infrastructure, including pipelines and storage tanks. Fiber-reinforced polymer composites, used in on-board vehicle storage tanks, offer strength and safety advantages due to their low permeability, high strength-to-weight ratio and avoiding hydrogen embrittlement issue.

Polymers like Nafion and Aquivion membranes are already used commercially in PEMWEs and fuel cells (PEMFCs). Nevertheless, ongoing research seeks to improve corrosion resistance, durability in harsh environments, and sustainability through non-fluorinated materials. ML and AI are accelerating materials development in this field.<sup>104</sup> Other commercial polymers currently used in hydrogen infrastructure are HDPE, PP, nylons (polyamides), silicone and fluorosilicone rubbers, EPDM, as pipelines, piping, seals and tubing.

Epoxy polymer composites reinforced with glass and carbon fibers are widely used in compressed hydrogen storage tanks for vehicles. However, large-scale adoption of hydrogen fuel requires improved tank design and failure analysis for enhanced safety. AI-assisted solutions,<sup>72,75</sup> particularly for Type IV & V all-polymer/polymer composite tanks, offer the potential to improve gravimetric energy density and eliminate hydrogen embrittlement seen in metal tanks. Innovations in thermoplastic composites are crucial for improving material recyclability at end-of-life, supporting long-term sustainability. Additionally, new polymers and coating with enhanced hydrogen barrier properties are needed for many of these applications. Hydrogen tanks face extreme temperature fluctuations, while emptying or emergency release of hydrogen lowering temperatures to  $-40\text{ }^{\circ}\text{C}$ , which can degrade the mechanical integrity of organic polymers, leading to brittleness.<sup>105</sup> Improvement of low temperature physical properties of such composites will benefit designing high-pressure storage tank and possibly enable the design of cryo-compressed and liquified tanks.

Porous polymer adsorbents for physical hydrogen storage, PHCs, polymer-based sensors are generally in low technology readiness level and require substantial improvement before their commercial use. Currently there is also no uniformity in reporting studies of hydrogen uptake by various adsorbents in terms of temperature and pressure. Performing and reporting gas absorption studies at practically relevant conditions (for example for automotive applications it is reported to be 298 K and 500 bar of pressure)<sup>41</sup> will help to lessen the development time and particularly advance the research area by enriching structure-property understanding of materials. On the other hand, polymers with selective hydrogen permeability are useful for gas purification and polymer-metal/metal hydride composite for hydrogen (chemical) storage application, which has much higher gravimetric energy density.

The combination of hydrogen and organic polymers need to be looked at cautiously because both are highly flammable. This can be addressed to some extent by choosing fire-retardant polymers/composites for this purpose such as fully aromatic poly(arylene ethers) and polyimides.

## Data availability

No primary research results, software or code have been included and no new data were generated or analysed as part of this review.

## Conflicts of interest

There are no conflicts to declare.

## Acknowledgements

This work was jointly funded by the National Research Foundation (NRF) and Agency for Science, Technology and Research (A\*STAR), Singapore for the RIE2025 Urban Solutions and Sustainability (USS) LCER Phase 2 Programme 1st Emerging Technology Grant Call (Grant no. U2411D4002).

## Notes and references

- (a) T. Terlouw, L. Rosa, C. Bauer and R. McKenna, *Nat. Commun.*, 2024, **15**, 7043; (b) M. van der Spek, C. Banet, C. Bauer, P. Gabrielli, W. Goldthorpe, M. Mazzotti, S. T. Munkejord, N. A. Røkke, N. Shah, N. Sunny, D. Sutter, J. M. Trusler and M. Gazzani, *Energy Environ. Sci.*, 2022, **15**, 1034–1077.
- (a) H. Zhang, Y. Fu, H. T. Nguyen, B. Fox, J. H. Lee, A. K.-T. Lau, H. Zheng, H. Lin, T. Ma and B. Jia, *Coord. Chem. Rev.*, 2023, **494**, 215272; (b) Center for Sustainable Systems, University of Michigan, Hydrogen Factsheet, <https://css.umich.edu/publications/factsheets/energy/hydrogen-factsheet>, 2024.
- A. M. Oliveira, R. R. Beswick and Y. Yan, *Curr. Opin. Chem. Eng.*, 2021, **33**, 100701.
- (a) Z. J. Baum, L. L. Diaz, T. Konovalova and Q. A. Zhou, *ACS Omega*, 2022, **7**, 32908–32935; (b) Q. Hassan, S. Algburi, A. Z. Sameen, H. M. Salman and M. Jaszczur, *Int. J. Hydrogen Energy*, 2024, **50**, 310–333.
- (a) *Achieving sustainable development with green hydrogen*, 2023, [https://gh2.org/sites/default/files/2023-05/GH2\\_Contracting%20Guidance\\_Sustainable%20development%20outcomes\\_v3%20%281%29\\_0.pdf](https://gh2.org/sites/default/files/2023-05/GH2_Contracting%20Guidance_Sustainable%20development%20outcomes_v3%20%281%29_0.pdf); (b) M. G. Rasul, M. A. Hazrat, M. A. Sattar, M. I. Jahirul and M. J. Shearer, *Energy Convers. Manage.*, 2022, **272**, 116326.
- N.-E. Laadel, M. El Mansori, N. Kang, S. Marlin and Y. Boussant-Roux, *Int. J. Hydrogen Energy*, 2022, **47**, 32707–32731.
- (a) D. Hauglustaine, F. Paulot, W. Collins, R. Derwent, M. Sand and O. Boucher, *Commun. Earth Environ.*, 2022, **3**, 295; (b) M. Sand, R. B. Skeie, M. Sandstad, S. Krishnan, G. Myhre, H. Bryant, R. Derwent, D. Hauglustaine, F. Paulot, M. Prather and D. Stevenson, *Commun. Earth Environ.*, 2023, **4**, 203.
- (a) H. Yu, J. Wan, M. Goodsite and H. Jin, *One Earth*, 2023, **6**, 267–277; (b) Y. Zhao, B. Jin, Y. Zheng, H. Jin, Y. Jiao and S.-Z. Qiao, *Adv. Energy Mater.*, 2018, **8**, 1801926; (c) H. Jin, Q. Gu, B. Chen, C. Tang, Y. Zheng, H. Zhang, M. Jaroniec and S.-Z. Qiao, *Chem*, 2020, **6**, 2382–2394; (d) R.-T. Liu, Z.-L. Xu, F.-M. Li, F.-Y. Chen, J.-Y. Yu, Y. Yan, Y. Chen and B. Y. Xia, *Chem. Soc. Rev.*, 2023, **52**, 5652–5683.
- A. Makhsoos, M. Kandidayeni, B. G. Pollet and L. Boulon, *Int. J. Hydrogen Energy*, 2023, **48**, 15341–15370.
- M. Carmo, D. L. Fritz, J. Mergel and D. Stolten, *Int. J. Hydrogen Energy*, 2013, **38**, 4901–4934.
- G. Wei, L. Xu, C. Huang and Y. Wang, *Int. J. Hydrogen Energy*, 2010, **35**, 7778–7783.
- C. J. Lee, J. Song, K. S. Yoon, Y. Rho, D. M. Yu, K.-H. Oh, J. Y. Lee, T.-H. Kim, Y. T. Hong, H.-J. Kim, S. J. Yoon and S. So, *J. Power Sources*, 2022, **518**, 230772.
- V. Antonucci, A. Di Blasi, V. Baglio, R. Ornelas, F. Matteucci, J. Ledesma-Garcia, L. G. Arriaga and A. S. Aricò, *Electrochim. Acta*, 2008, **53**, 7350–7356.



- 14 T. Kim, Y. Sihm, I.-H. Yoon, S. J. Yoon, K. Lee, J. H. Yang, S. So and C. W. Park, *ACS Appl. Nano Mater.*, 2021, **4**, 9104–9112.
- 15 D. Aili, M. K. Hansen, C. Pan, Q. Li, E. Christensen, J. O. Jensen and N. J. Bjerrum, *Int. J. Hydrogen Energy*, 2011, **36**, 6985–6993.
- 16 S. Siracusano, V. Baglio, F. Lufrano, P. Staiti and A. S. Arico, *J. Membr. Sci.*, 2013, **448**, 209–214.
- 17 C. Klose, T. Saatkamp, A. Münchinger, L. Bohn, G. Titvinidze, M. Breitwieser, K.-D. Kreuer and S. Vierrath, *Adv. Energy Mater.*, 2020, **10**, 1903995.
- 18 F. N. Khatib, T. Wilberforce, O. Ijaodola, E. Ogungbemi, Z. El-Hassan, A. Durrant, J. Thompson and A. G. Olabi, *Renewable Sustainable Energy Rev.*, 2019, **111**, 1–14.
- 19 Q. Feng, X. Z. Yuan, G. Liu, B. Wei, Z. Zhang, H. Li and H. Wang, *J. Power Sources*, 2017, **366**, 33–55.
- 20 S. Weidner, M. Faltenbacher, I. François, D. Thomas, J. B. Skúlason and C. Maggi, *Int. J. Hydrogen Energy*, 2018, **43**, 15625–15638.
- 21 U. Babic, M. Suermann, F. N. Büchi, L. Gubler and T. J. Schmidt, *J. Electrochem. Soc.*, 2017, **164**, F387.
- 22 P. Millet, D. Dragoe, S. Grigoriev, V. Fateev and C. Etievant, *Int. J. Hydrogen Energy*, 2009, **34**, 4974–4982.
- 23 N. S. Hassan, A. A. Jalil, S. Rajendran, N. F. Khusnun, M. B. Bahari, A. Johari, M. J. Kamaruddin and M. Ismail, *Int. J. Hydrogen Energy*, 2024, **52**, 420–441.
- 24 W. Nie, M. Ruan, X. Liu, K. Ruan, Y. Sun and Z. Liu, *Chem. Eng. J.*, 2024, **480**, 148321.
- 25 S. Pal, P. S. Das, M. K. Naskar and S. Ghosh, *Mater. Today Sustainability*, 2024, **25**, 100610.
- 26 T. Takayama, A. Iwase and A. Kudo, *ACS Appl. Mater. Interfaces*, 2024, **16**, 36423–36432.
- 27 T. Banerjee, F. Podjaski, J. Kröger, B. P. Biswal and B. V. Lotsch, *Nat. Rev. Mater.*, 2021, **6**, 168–190.
- 28 R. S. Sprick, J.-X. Jiang, B. Bonillo, S. Ren, T. Ratvijitvech, P. Guignon, M. A. Zwijnenburg, D. J. Adams and A. I. Cooper, *J. Am. Chem. Soc.*, 2015, **137**, 3265–3270.
- 29 S. Ghosh, N. A. Kouamé, L. Ramos, S. Remita, A. Dazzi, A. Deniset-Besseau, P. Beaunier, F. Goubard, P.-H. Aubert and H. Remita, *Nat. Mater.*, 2015, **14**, 505–511.
- 30 C. Pornrungroj, M. Ozawa, T. Onodera and H. Oikawa, *RSC Adv.*, 2018, **8**, 38773–38779.
- 31 C. Yang, B. Cheng, J. Xu, J. Yu and S. Cao, *EnergyChem*, 2024, **6**, 100116.
- 32 Z. Zhang, X. Chen, H. Zhang, W. Liu, W. Zhu and Y. Zhu, *Adv. Mater.*, 2020, **32**, 1907746.
- 33 J. Jiang, K. Kato, H. Fujimori, A. Yamakata and Y. Sakata, *J. Catal.*, 2020, **390**, 81–89.
- 34 S. Wei, X. Xia, S. Bi, S. Hu, X. Wu, H.-Y. Hsu, X. Zou, K. Huang, D. W. Zhang, Q. Sun, A. J. Bard, E. T. Yu and L. Ji, *Chem. Soc. Rev.*, 2024, **53**, 6860–6916.
- 35 (a) K. Ranganathan and A. Parthiban, *Polymer*, 2018, **135**, 295–304; (b) K. Ranganathan and P. Anbanandam, *Polym. Chem.*, 2015, **6**, 4560–4564; (c) A. Parthiban and K. Ranganathan, *J. Fluorine Chem.*, 2016, **191**, 70–76.
- 36 P. M. Budd, B. S. Ghanem, S. Makhseed, N. B. McKeown, K. J. Msayib and C. E. Tattershall, *Chem. Commun.*, 2004, 230–231, DOI: [10.1039/B311764B](https://doi.org/10.1039/B311764B).
- 37 D. Ramimoghadam, S. E. Boyd, C. L. Brown, E. Mac, A. Gray and C. J. Webb, *ChemPhysChem*, 2019, **20**, 1613–1623.
- 38 K. Polak-Kraśna, R. Dawson, L. T. Holyfield, C. R. Bowen, A. D. Burrows and T. J. Mays, *J. Mater. Sci.*, 2017, **52**, 3862–3875.
- 39 S. Rochat, K. Polak-Kraśna, M. Tian, T. J. Mays, C. R. Bowen and A. D. Burrows, *Int. J. Hydrogen Energy*, 2019, **44**, 332–337.
- 40 M. Tian, S. Rochat, H. Fawcett, A. D. Burrows, C. R. Bowen and T. J. Mays, *Adsorption*, 2020, **26**, 1083–1091.
- 41 T. G. Voskuilen, T. L. Pourpoint and A. M. Dailly, *Adsorption*, 2012, **18**, 239–249.
- 42 S. Rochat, K. Polak-Kraśna, M. Tian, L. T. Holyfield, T. J. Mays, C. R. Bowen and A. D. Burrows, *J. Mater. Chem. A*, 2017, **5**, 18752–18761.
- 43 L. Y. Molefe, N. M. Musyoka, J. Ren, H. W. Langmi, P. G. Ndungu, R. Dawson and M. Mathe, *J. Mater. Sci.*, 2019, **54**, 7078–7086.
- 44 B. Li, X. Huang, R. Gong, M. Ma, X. Yang, L. Liang and B. Tan, *Int. J. Hydrogen Energy*, 2012, **37**, 12813–12820.
- 45 L. Yang, Y. Ma, Y. Xu and G. Chang, *Chem. Commun.*, 2019, **55**, 11227–11230.
- 46 D. Xu, L. Sun, G. Li, J. Shang, R.-X. Yang and W.-Q. Deng, *Chem. – Eur. J.*, 2016, **22**, 7944–7949.
- 47 M. C. Kreider, M. Sefa, J. A. Fedchak, J. Scherschligt, M. Bible, B. Natarajan, N. N. Klimov, A. E. Miller, Z. Ahmed and M. R. Hartings, *Polym. Adv. Technol.*, 2018, **29**, 867–873.
- 48 (a) M.-J. Zhou, Y. Miao, Y. Gu and Y. Xie, *Adv. Mater.*, 2024, **36**, 2311355; (b) V. Sage, J. Patel, P. Hazewinkel, Q. U. A. Yasin, F. Wang, Y. Yang, K. Kozielski and C. E. Li, *Int. J. Hydrogen Energy*, 2024, **56**, 1419–1434; (c) A. Lin and G. Bagnato, *Int. J. Hydrogen Energy*, 2024, **63**, 315–329.
- 49 (a) H. Staudinger, E. Geiger and E. Huber, *Ber. Dtsch. Chem. Ges. A*, 1929, **62**, 263–267; (b) R. Mülhaupt, *Angew. Chem., Int. Ed.*, 2004, **43**, 1054–1063; (c) R. Kato and H. Nishide, *Polym. J.*, 2018, **50**, 77–82.
- 50 R. Kato, K. Yoshimasa, T. Egashira, T. Oya, K. Oyaizu and H. Nishide, *Nat. Commun.*, 2016, **7**, 13032.
- 51 R. Kato, K. Oka, K. Yoshimasa, M. Nakajima, H. Nishide and K. Oyaizu, *Macromol. Rapid Commun.*, 2019, **40**, 1900139.
- 52 K. Oka, Y. Kaiwa, M. Kataoka, K.-I. Fujita and K. Oyaizu, *Eur. J. Org. Chem.*, 2020, 5876–5879.
- 53 R. Kato, T. Oya, Y. Shimazaki, K. Oyaizu and H. Nishide, *Polym. Int.*, 2017, **66**, 647–652.
- 54 (a) R. Yamaguchi, C. Ikeda, Y. Takahashi and K.-I. Fujita, *J. Am. Chem. Soc.*, 2009, **131**, 8410–8412; (b) S. Chakraborty, W. W. Brennessel and W. D. Jones, *J. Am. Chem. Soc.*, 2014, **136**, 8564–8567.
- 55 (a) Y. Kaiwa, K. Oka, H. Nishide and K. Oyaizu, *Polym. Adv. Technol.*, 2021, **32**, 1162–1167; (b) K. Oka, Y. Kaiwa, S. Furukawa, H. Nishide and K. Oyaizu, *ACS Appl. Polym. Mater.*, 2020, **2**, 2756–2760.
- 56 K. Oka, M. Kataoka, H. Nishide and K. Oyaizu, *MRS Commun.*, 2022, **12**, 213–216.
- 57 (a) K. Oka, Y. Tobita, M. Kataoka, S. Murao, K. Kobayashi, S. Furukawa, H. Nishide and K. Oyaizu, *Polym. J.*, 2021, **53**, 799–804; (b) K. Oka, Y. Tobita, M. Kataoka, K. Kobayashi, Y. Kaiwa, H. Nishide and K. Oyaizu, *Polym. Int.*, 2022, **71**, 348–351; (c) K. Oka, Y. Kaiwa, K. Kobayashi, Y. Tobita and K. Oyaizu, *Polym. Chem.*, 2023, **14**, 2588–2591.
- 58 K. Oyaizu, *Polym. J.*, 2024, **56**, 127–144.
- 59 H. Nishide, *Green Chem.*, 2022, **24**, 4650–4679.
- 60 M. Sharifian, W. Kern and G. Riess, *Polymers*, 2022, **14**, 4512.
- 61 (a) L. Liu, A. Ilyushechkin, D. Liang, A. Cousins, W. Tian, C. Chen, J. Yin and L. Schoeman, *Inorganics*, 2023, **11**, 181; (b) R. Bardhan, A. M. Ruminski, A. Brand and J. J. Urban, *Energy Environ. Sci.*, 2011, **4**, 4882–4895.
- 62 (a) L. Schlapbach and A. Züttel, *Nature*, 2001, **414**, 353–358; (b) A. Schneemann, J. L. White, S. Kang, S. Jeong, L. F. Wan, E. S. Cho, T. W. Heo, D. Prendergast, J. J. Urban, B. C. Wood, M. D. Allendorf and V. Stavila, *Chem. Rev.*, 2018, **118**, 10775–10839.
- 63 G. R. d Almeida Neto, F. H. Matheus, C. A. Gonçalves Beatrice, D. R. Leiva and L. A. Pessan, *Int. J. Hydrogen Energy*, 2022, **47**, 34139–34164.
- 64 (a) E. S. Cho, F. Qiu and J. J. Urban, *Small*, 2017, **13**, 1602572; (b) K.-J. Jeon, H. R. Moon, A. M. Ruminski, B. Jiang, C. Kisielowski, R. Bardhan and J. J. Urban, *Nat. Mater.*, 2011, **10**, 286–290.
- 65 K. Kubo, Y. Kawaharazaki and H. Itoh, *Int. J. Hydrogen Energy*, 2017, **42**, 22475–22479.
- 66 The energy density of hydrogen, <https://demaco-cryogenics.com/blog/energy-density-of-hydrogen/>.
- 67 Hydrogen Storage, <https://www.energy.gov/eere/fuelcells/hydrogen-storage>.
- 68 H. Yu, A. Diaz, X. Lu, B. Sun, Y. Ding, M. Koyama, J. He, X. Zhou, A. Oudriss, X. Feaugas and Z. Zhang, *Chem. Rev.*, 2024, **124**, 6271–6392.
- 69 Y. Li, F. Barzagli, P. Liu, X. Zhang, Z. Yang, M. Xiao, Y. Huang, X. Luo, C. E. Li, H. A. Luo and R. Zhang, *Ind. Eng. Chem. Res.*, 2023, **62**, 15752–15773.
- 70 R. R. Barth, K. L. Simmons and C. W. San Marchi, *Polymers for hydrogen infrastructure and vehicle fuel systems*, United States, 2013.
- 71 M. Nachtane, M. Tarfaoui, M. A. Abichou, A. Vetcher, M. Rouway, A. Aâmir, H. Mouadili, H. Laaouidi and H. Naanani, *J. Compos. Sci.*, 2023, **7**, 119.
- 72 J. Keyte, K. Pancholi and J. Njuguna, *Front. Mater.*, 2019, **6**, 224.
- 73 W. Gul, Y. E. Xia, P. Gérard and S. K. Ha, *Polymers*, 2023, **15**, 3716.
- 74 (a) M. Kumar, *Int. J. Pressure Vessels Piping*, 2024, **208**, 105150; (b) R. R. Patil, R. K. Calay, M. Y. Mustafa and S. Thakur, *Hydrogen*, 2024, **5**, 312–326.



- 75 (a) J. Condé-Wolter, M. G. Ruf, A. Liebsch, T. Lebelt, I. Koch, K. Drechsler and M. Gude, *Composites, Part A*, 2023, **167**, 107446; (b) W. Balasooriya, C. Clute, B. Schrittmesser and G. Pinter, *Polym. Rev.*, 2022, **62**, 175–209.
- 76 E. Scgambitterra and L. Pagnotta, *Energies*, 2024, **17**, 2216.
- 77 (a) C. Habel, E. S. Tsurko, R. L. Timmins, J. Hutschreuther, R. Kunz, D. D. Schuchardt, S. Rosenfeldt, V. Altstädt and J. Brey, *ACS Nano*, 2020, **14**, 7018–7024; (b) M.-H. Klopffer, P. Berne and É. Espuche, *Oil Gas Sci. Technol.*, 2015, **70**, 305–315; (c) Y. Lei, L. Liu, C. A. Scholes and S. E. Kentish, *Int. J. Hydrogen Energy*, 2024, **54**, 947–954.
- 78 H. Kanesugi, K. Ohyama, H. Fujiwara and S. Nishimura, *Int. J. Hydrogen Energy*, 2023, **48**, 723–739.
- 79 S. Yuan, Y. Sun, C. Yang, Y. Zhang, C. Cong, Y. Yuan, D. Lin, L. Pei, Y. Zhu and H. Wang, *Chem. Eng. J.*, 2022, **449**, 137876.
- 80 (a) M. Liu, K. Lin, M. Zhou, A. Wallwork, M. A. Bissett, R. J. Young and I. A. Kinloch, *Compos. Sci. Technol.*, 2024, **249**, 110483; (b) R. Moran, Less hydrogen gas leakage: graphene polymers for the hydrogen economy, <https://graphene-flagship.eu/materials/news/less-hydrogen-gas-leakage-graphene-polymers-for-the-hydrogen-economy/>, (accessed 10 October, 2024); (c) S. Yuan, Y. Sun, C. Cong, Y. Liu, D. Lin, L. Pei, Y. Zhu and H. Wang, *Carbon*, 2023, **205**, 54–68.
- 81 (a) Y.-H. Yang, L. Bolling, M. A. Priolo and J. C. Grunlan, *Adv. Mater.*, 2013, **25**, 493; (b) P. Tzeng, B. Stevens, I. Devlaming and J. C. Grunlan, *Langmuir*, 2015, **31**, 5919–5927; (c) X. Li, P. Bandyopadhyay, T. T. Nguyen, O.-K. Park and J. H. Lee, *J. Membr. Sci.*, 2018, **547**, 80–92; (d) X. Li, P. Bandyopadhyay, M. Guo, N. H. Kim and J. H. Lee, *Carbon*, 2018, **133**, 150–161.
- 82 O. B. Seo, S. Saha, N. H. Kim and J. H. Lee, *J. Membr. Sci.*, 2021, **640**, 119839.
- 83 J. Miyake, Y. Ogawa, T. Tanaka, J. Ahn, K. Oka, K. Oyaizu and K. Miyatake, *Commun. Chem.*, 2020, **3**, 138.
- 84 J. Miyake, T. Watanabe, H. Shintani, Y. Sugawara, M. Uchida and K. Miyatake, *ACS Mater. Au*, 2021, **1**, 81–88.
- 85 A. Salehabadi, N. Ismail, N. Morad, M. Rafatullah and M. Idayu Ahmad, *Int. J. Energy Res.*, 2021, **45**, 4026–4035.
- 86 J. Guan, X. Sun, H. Yu, J. Zheng, Y. Sun, S. Li, G. Qin and S. Zhang, *J. Membr. Sci.*, 2024, **700**, 122664.
- 87 R. Rath, P. Kumar, L. Unnikrishnan, S. Mohanty and S. K. Nayak, *Mater. Chem. Phys.*, 2021, **260**, 124148.
- 88 P. Qian, L. Li, H. Wang, J. Sheng, Y. Zhou and H. Shi, *J. Membr. Sci.*, 2022, **662**, 120973.
- 89 L. Liu, L. Bai, Z. Liu, S. Miao, J. Pan, L. Shen, Y. Shi and N. Li, *J. Membr. Sci.*, 2023, **665**, 121135.
- 90 Q. Liu, S. Zhang, L. Tian, J. Li, W. Ma, F. Wang, Z. Wang, J. Li and H. Zhu, *J. Power Sources*, 2023, **564**, 232822.
- 91 W. W. Gou, W. T. Gao, X. L. Gao, Q. G. Zhang, A. M. Zhu and Q. L. Liu, *J. Membr. Sci.*, 2022, **645**, 120200.
- 92 C. Hu, J. H. Park, H. M. Kim, H. H. Wang, J. Y. Bae, N. Y. Kang, N. Chen and Y. M. Lee, *J. Membr. Sci.*, 2022, **647**, 120341.
- 93 J. J. Wang, W. T. Gao, Y. S. L. Choo, Z. H. Cai, Q. G. Zhang, A. M. Zhu and Q. L. Liu, *J. Colloid Interface Sci.*, 2023, **629**, 377–387.
- 94 (a) P. S. Chauhan and S. Bhattacharya, *Int. J. Hydrogen Energy*, 2019, **44**, 26076–26099; (b) E. Gorbova, G. Balkourani, C. Molochas, D. Sidiropoulos, A. Brouzgou, A. Demin and P. Tsiakaras, *Catalysts*, 2022, **12**, 1647.
- 95 H. Gu, Z. Wang and Y. Hu, *Sensors*, 2012, **12**, 5517–5550.
- 96 K. Ramaiyan, L.-k Tsui, E. L. Brosha, C. Kreller, J. R. Stetter, T. Russ, W. Du, D. Peaslee, G. Hunter, J. Xu, D. Makel, F. Garzon and R. Mukundan, *ECS Sens. Plus*, 2023, **2**, 045601.
- 97 W.-T. Koo, Y. Kim, S. Kim, B. L. Suh, S. Savagatrup, J. Kim, S.-J. Lee, T. M. Swager and I.-D. Kim, *Chem*, 2020, **6**, 2746–2758.
- 98 K. Arora, S. Srivastava, P. R. Solanki and N. K. Puri, *IEEE Sens. J.*, 2019, **19**, 8262–8271.
- 99 W. Li, L. Huang, H. Sun, B. Wang, Q. Lu, X. Liang, F. Liu, F. Liu, P. Sun and G. Lu, *Sens. Actuators, B*, 2022, **366**, 132014.
- 100 S.-W. Jung, E. K. Lee, J. H. Kim and S.-Y. Lee, *Solid State Ionics*, 2020, **344**, 115134.
- 101 S.-H. Hwang, Y. K. Kim, S. M. Jeong, C. Choi, K. Y. Son, S.-K. Lee and S. K. Lim, *Text. Res. J.*, 2020, **90**, 2198–2211.
- 102 W. Small, D. J. Maitland, T. S. Wilson, J. P. Bearinger, S. A. Letts and J. E. Trebes, *Sens. Actuators, B*, 2009, **139**, 375–379.
- 103 D. Kanzhigitova, P. Askar, A. Tapkharov, V. Kudryashov, M. Abutalip, R. Rakhmetullayeva, S. Adilov and N. Nuraje, *Adv. Compos. Hybrid Mater.*, 2023, **6**, 218.
- 104 (a) R. Ding, Y. Ding, H. Zhang, R. Wang, Z. Xu, Y. Liu, W. Yin, J. Wang, J. Li and J. Liu, *J. Mater. Chem. A*, 2021, **9**, 6841–6850; (b) R. Ding, S. Zhang, Y. Chen, Z. Rui, K. Hua, Y. Wu, X. Li, X. Duan, X. Wang, J. Li and J. Liu, *Energy AI*, 2022, **9**, 100170; (c) A. Mohamed, H. Ibrahim and K. Kim, *Energy Rep.*, 2022, **8**, 13425–13437; (d) Y. Bai, L. Wilbraham, B. J. Slater, M. A. Zwijnenburg, R. S. Sprick and A. I. Cooper, *J. Am. Chem. Soc.*, 2019, **141**, 9063–9071.
- 105 L. Zhao, Q. Zhao, J. Zhang, S. Zhang, G. He, M. Zhang, T. Su, X. Liang, C. Huang and W. Yan, *Int. J. Hydrogen Energy*, 2021, **46**, 22554–22573.

